World Academy of Science, Engineering and Technology
International Journal of Mechanical and Mechatronics Engineering
Vol:10, No:8, 2016

Effect of Loop Diameter, Height and Insulation on a High Temperature CO_2 Based Natural Circulation Loop

S. Sadhu, M. Ramgopal, S. Bhattacharyya

***Abstract*—**Natural circulation loops (NCLs) are buoyancy driven flow systems without any moving components. NCLs have vast applications in geothermal, solar and nuclear power industry where reliability and safety are of foremost concern. Due to certain favorable thermophysical properties, especially near supercritical regions, carbon dioxide can be considered as an ideal loop fluid in many applications. In the present work, a high temperature NCL that uses supercritical carbon dioxide as loop fluid is analysed. The effects of relevant design and operating variables on loop performance are studied. The system operating under steady state is modelled taking into account the axial conduction through loop fluid and loop wall, and heat transfer with surroundings. The heat source is considered to be a heater with controlled heat flux and heat sink is modelled as an end heat exchanger with water as the external cold fluid. The governing equations for mass, momentum and energy conservation are normalized and are solved numerically using finite volume method. Results are obtained for a loop pressure of 90 bar with the power input varying from 0.5 kW to 6.0 kW. The numerical results are validated against the experimental results reported in the literature in terms of the modified Grashof number (Gr_m) and Reynolds number (Re). Based on the results, buoyancy and friction dominated regions are identified for a given loop. Parametric analysis has been done to show the effect of loop diameter, loop height, ambient temperature and insulation. The results show that for the high temperature loop, heat loss to surroundings affects the loop performance significantly. Hence this conjugate heat transfer between the loop and surroundings has to be considered in the analysis of high temperature NCLs.

***Keywords*—**Conjugate heat transfer, heat loss, natural circulation loop, supercritical carbon dioxide.

NOMENCLATURE

A	Heat transfer surface area (m^2)
C_p	Specific heat (J kg^{-1} K^{-1})
d	Diameter (m)
f	Friction factor
G	Mass flux (kg m^{-2} s^{-1})
g	Acceleration due to gravity (ms^{-2})
h	Heat transfer coefficient (W m^{-2} K^{-1})
H	Height (m)
L	Length (m)
p	Pressure (N m^{-2})
$\dot{Q}$	Power (W m^{-2})
R	Area Ratio
T	Temperature (K)
t	Time (s)
U	Velocity (ms^{-1})
Uo	Overall heat transfer coefficient (W m^{-2} K^{-1})
V	Volume (m^3)
W	Mass flow rate (kg s^{-1})
z	Length in axial direction (m)
Gr_m	Modified Grashof number
Gz	Graetz number
Nu	Nusselt number
Pr	Prandtl number
Ra	Rayleigh number
Re	Reynolds number
St_m	Modified Stanton number

Greek Symbol

β	Volumetric expansion coefficient (K^{-1})
ρ	Density (kg m^{-3})
λ	Thermal conductivity (W m^{-1} K^{-1})
μ	Dynamic Viscosity (kg m^{-1} s^{-1})
θ	Non-dimensional temperature
ϕ	Flow direction angle with vertical (anticlockwise +ve)
τ	Non-dimensional time
δ	Thickness (m)
ε	Effectiveness

Superscript and subscript

t	total
d	diameter
f	fluid
h	heater
w	wall
c	cooler
i	inner
o	outer
ex	external
ss	steady-state
ref	reference
cs	cross-sectional
av	average
a	air
ins	insulation

Abbreviation

TTD	Terminal temperature difference
NCL	Natural Circulation Loop

S. Sadhu is with the is with the Mechanical Engineering Department, Indian Institute of Technology Kharagpur, Kharagpur 721302 India (phone: +91-7076607339, e-mail: sayan.jupower@gmail.com).

M. Ramgopal and S. Bhattacharyya are with the Mechanical Engineering Department, Indian Institute of Technology Kharagpur, Kharagpur 721302 India (e-mail: ramg@mech.iitkgp.ernet.in, souvik.iit@gmail.com).

I. INTRODUCTION

IN the last two decades, carbon dioxide has witnessed growing popularity as a secondary fluid in forced, as well as NCLs, due to its favourable thermo-physical properties and

ecologically benign nature [11], [14]. NCLs offer certain advantages over forced circulation loops and are preferred, particularly where safety is of foremost concern, for example, in nuclear power plants. NCLs are also widely used in applications such as refrigeration and air conditioning systems, solar collectors, geothermal heat pumps, cryogenic systems, chemical extraction and electronic cooling systems, etc. Studies show that for low temperature refrigeration and air conditioning applications, use of CO_2 in place of conventional secondary fluids results in very compact loops [11]. CO_2 based NCLs have also been proposed for various heat transfer applications such as new generation nuclear reactors [24], in chemical extraction [7], [19], cryogenic refrigeration [9], [16], heat pump [13], electronic cooling systems [4], geothermal applications [3], [10], etc. Comprehensive review of NCL is done by Zvirin [27], Isshi and Kataoka [17] describe the scaling analysis of the loop. Stability analysis of NCL is done extensively [22], [2]. However, detailed modelling and analyses of CO_2 based NCLs are relatively sparse in the literature. Kumar and Ramgopal reported a one-dimensional steady-state analysis of a rectangular NCL with end heat exchangers for low temperature applications [12] followed by 3D simulation by Yadav et al [1]. Zhang et al. [26] and Chen et al. [15] reported studies on the effects of heat transfer and the instabilities of supercritical CO_2 flow in a 2-D NCL at a fixed operating pressure of 90 bar operating over a large heat source temperature range. Experimental analysis of a mini loop is done [18]. Most of the studies available for CO_2 based NCLs are for isothermal heat source and sink, which has less practical significance than NCLs with end heat exchangers.

Also review of the literature shows that most of the CO_2 based NCLs employing1-D models considered adiabatic riser and downcomer section neglecting heat loss to the ambient and axial conduction. Though heat loss may not be important for loops operating near ambient temperature, this can affect the performance significantly for high temperature loops as properties vary drastically near the critical region. Also studies on high temperature supercritical CO_2 loops with constant heat flux heating and an end heat exchanger have not been reported in open literature. To fill in that void, this study presents a numerical analysis of supercritical CO_2 based NCL with constant heat flux heat source and cold end heat exchanger sink. The operating parameter range is chosen such that the loop fluid (CO_2) always exists as a supercritical single-phase fluid. Parametric analyses are conducted to study the effect of loop geometry, insulation and ambient temperature.

II. Physical Model and Mathematical Formulations

A. Physical Model

In the present study, a rectangular NCL has been considered (Fig. 1). Circulation of the loop fluid is maintained due to the buoyancy effect caused by heating at the bottom and cooling at the top. The loop fluid is assumed to be heated by a constant heat flux heat source placed at the bottom horizontal arm (4-1) and the fluid is cooled by a counter-flow tube-in-tube type heat exchanger placed at the top horizontal arm (2-3). Both the source and sink are considered to be perfectly insulated from the ambient, which implies that only mode of energy interaction possible is heat transfer with the loop wall. However, the vertical arms and un-insulated portions of the horizontal arms (1-2 and 3-4) are subjected to heat loss to the cooler ambient air. Supercritical carbon dioxide (CO_2) is considered to be the primary working fluid flowing through the loop and water is the coolant fluid flowing through the annular passage of the tube-in tube type heat exchanger.

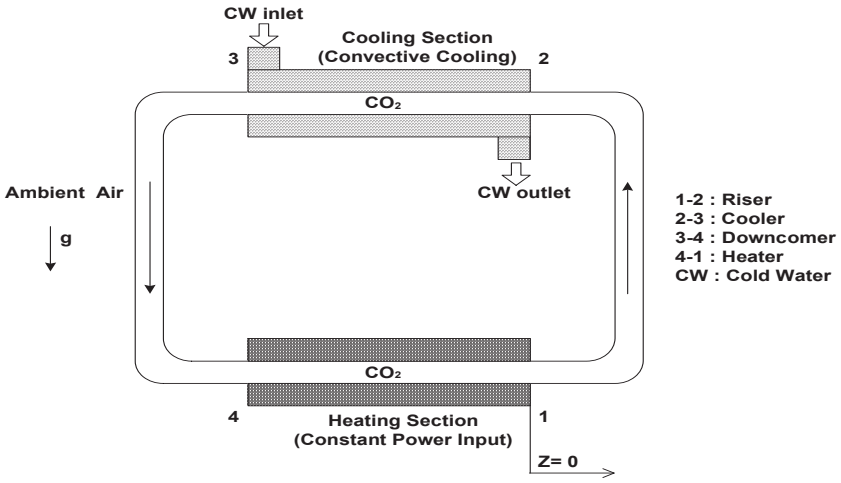

Fig. 1 Physical model of the rectangular NCL

B. Assumptions

The following simplifying assumptions have been made:

1. The loop is assumed to be operating under steady state.
2. Fluid properties are assumed to vary in axial direction.
3. Boussinesq approximation is valid for flow of CO_2.
4. Viscous dissipation is neglected in the energy equation.
5. Minor losses in the pipe bends are neglected.
6. Properties of wall material are considered at average wall temperature.

C. Governing Equations

1. Loop Fluid

One-dimensional conservation of mass equation for the loop fluid flowing through a tube of constant circular cross-section can be written as:

$$\frac{\partial \rho_f}{\partial t} + \frac{\partial G_f}{\partial z} = 0 \tag{1}$$

1-D momentum balance equation for loop fluid flowing in through a tube of constant circular cross-section can be written as,

$$\frac{\partial G_f}{\partial t} + \frac{\partial}{\partial z}\left(\frac{G_f{}^2}{\rho_f}\right) = -\frac{\partial p}{\partial z} + \frac{f_i}{2d_i}\left(\frac{G_f{}^2}{\rho_f}\right) - \rho_f g Cos\,\phi \tag{2}$$

Similarly, 1-Dconservation of energy equations for the loop fluid is written as:

$$\rho_f C_{pf}\frac{\partial T_f}{\partial t} + G_f C_{pf}\frac{\partial T_f}{\partial z} = \frac{\partial}{\partial z}\left(\lambda_f \frac{\partial T_f}{\partial z}\right) - \left(\frac{4}{d_i}\right)h_i\left(T_f - T_w\right) \tag{3}$$

The first term on the right-hand side of (3) represents the axial conduction within the fluid itself and the second term shows the convective contribution from the wall. The loop fluid is in contact with the wall material only, not with the source or the sink directly, and hence energy interaction is solely via convection with the wall. The direction of heat transfer depends on the sign of temperature difference between the wall and the fluid.

$$G_f = \frac{W_f}{A_i} \tag{4}$$

Using Boussinesq approximation, the density is given by:

$$\rho_f = \rho_{ref}\left[1 + \beta\left(T_{ref} - T\right)\right] \tag{5}$$

As NCL is driven by buoyancy with no other external factors, the cyclic integral of the fluid momentum equation around the total loop length is given by:

$$\oint \Delta p = 0 \tag{6}$$

$$L_t\frac{dG_f}{dt} + \left(\frac{f_i L_t}{2d_i}\right)\left(\frac{G_f{}^2}{\rho_f}\right) + \rho_f g Cos\,\phi\beta_{av}\oint\left(T_{ref} - T\right)dz = 0 \tag{7}$$

Coolant inlet temperature is expected to be the lowest in the system and hence that has been chosen as the reference temperature. All fluid properties depend on local temperatures and hence both the buoyancy and frictional terms need to be estimated on local basis.

2. Tube Wall

The tube wall is subjected to different kinds of energy interactions in different sections of the loop. It receives constant power heat input in the heater section (4-1), rejects heat via convective heat transfer to cooling water in the cooler section (2-3) and also loses heat via convective heat transfer to ambient air along other un-insulated sections such as riser (1-2) and downcomer (3-4). It also exchanges heat with the loop fluid along entire length of the loop (L_t). Hence the energy equation for the wall can be expressed as:

For heater section (4-1):

$$\rho_w C_{pw}\frac{\partial T_w}{\partial t} = \frac{\partial}{\partial z}\left(\lambda_w\frac{\partial T_w}{\partial z}\right) - \left(\frac{A_i}{V_w}\right)h_i\left(T_w - T_f\right) + \frac{\dot{Q}}{V_w} \tag{8a}$$

For cooler section (2-3):

$$\rho_w C_{pw}\frac{\partial T_w}{\partial t} = \frac{\partial}{\partial z}\left(\lambda_w\frac{\partial T_w}{\partial z}\right) - \left(\frac{A_i}{V_w}\right)h_i\left(T_w - T_f\right) + \left(\frac{A_o}{V_w}\right)h_{ex}\left(T_w - T_c\right) \tag{8b}$$

For riser (1-2) and downcomer (3-4) section:

$$\rho_w C_{pw}\frac{\partial T_w}{\partial t} = \frac{\partial}{\partial z}\left(\lambda_w\frac{\partial T_w}{\partial z}\right) - \left(\frac{A_i}{V_w}\right)h_i\left(T_w - T_f\right) + \left(\frac{A_o}{V_w}\right)h_a\left(T_w - T_a\right) \tag{8c}$$

3. Coolant

Temperature profile of the coolant stream can be obtained by simultaneously solving the associated energy equation, expressed as:

$$\rho_c C_{pc}\frac{\partial T_c}{\partial t} + G_c C_{pc}\frac{\partial T_c}{\partial z} = \frac{\partial}{\partial z}\left(\lambda_c\frac{\partial T_c}{\partial z}\right) + \left(\frac{A_o}{V_c}\right)h_{ex}\left(T_w - T_c\right) \tag{9}$$

D. Non-Dimensionalization of Governing Equations for System under Steady State

The governing equations for the loop operating under steady state are non-dimensionalised using suitable reference parameters.

$$\begin{aligned}
&\hat{z} = \frac{z}{L_t}, \hat{G} = \frac{G}{G_{ss}}, G_{ss} = \frac{W_{ss}}{A_{cs}}, U_{ss} = \frac{G_{ss}}{\rho_{ref}},\\
&\theta = \frac{T - T_{ref}}{\Delta T_{ref}}, \Delta T_{ref} = \frac{\dot{Q}}{G_{ss}A_{cs}C_{pref}},\\
&\hat{\rho} = \frac{\rho}{\rho_{ref}}, \hat{\mu} = \frac{\mu}{\mu_{ref}}, \hat{C}_p = \frac{C_p}{C_{pref}}, \hat{\lambda} = \frac{\lambda}{\lambda_{ref}}
\end{aligned} \tag{10}$$

4. Loop Fluid

Now, by using the above-mentioned non-dimensional parameters (10), the momentum (7) and energy (3) equation of the loop fluid in steady state can be written as:

$$\left(\frac{f_i L_t}{2d_i}\right)\left(\frac{\hat{G}_f{}^2}{\hat{\rho}_f}\right) - \left(\frac{L_t}{H}\right)\frac{Gr_m}{\mathrm{Re}_{ss}^3}\oint\theta\hat{g}_z Cos\,\phi d\hat{z} = 0 \tag{11}$$

$$\hat{G}_f \hat{C}_{pf} \frac{\partial \theta_f}{\partial \hat{z}} = \left(\frac{d_i}{L_t}\right) \frac{1}{\mathrm{Re}_{ss}\,\mathrm{Pr}_{ref}} \frac{\partial}{\partial \hat{z}} \left(\hat{\lambda}_f \frac{\partial \theta_f}{\partial \hat{z}}\right) - St_{mi}\left(\theta_f - \theta_w\right) \quad (12)$$

where, $\hat{g}_z Cos\,\phi$ represents the direction of gravity force along loop length. For the riser, its value is +1 $\left(\phi = 0^o\right)$, for the downcomer it is −1 $\left(\phi = 180^o\right)$ and for horizontal arms it is 0 $\left(\phi = \pm 90^o\right)$.

5. Tube Wall

Similarly, the different forms of wall energy equation (8a), (8b), and (8c) in steady state can be written as,

For heater section (4-1):

$$0 = \left(\frac{d_i}{L_t}\right) \frac{1}{\mathrm{Re}_{ss}\,\mathrm{Pr}_{ref}} \frac{\partial}{\partial \hat{z}} \left(\hat{\lambda}_w \frac{\partial \theta_w}{\partial \hat{z}}\right) - St_{mi} R_i \left(\theta_w - \theta_f\right) + \frac{\dot{Q} R_i}{G_{ss} A_{cs} C_{pref} \Delta T_{ref}} \left(\frac{L_t}{L_h}\right) \quad (13a)$$

For cooler section (2-3):

$$0 = \left(\frac{d_i}{L_t}\right) \frac{1}{\mathrm{Re}_{ss}\,\mathrm{Pr}_{ref}} \frac{\partial}{\partial \hat{z}} \left(\hat{\lambda}_w \frac{\partial \theta_w}{\partial \hat{z}}\right) - St_{mi} R_i \left(\theta_w - \theta_f\right) - St_{mex} R_o \left(\theta_w - \theta_c\right) \quad (13b)$$

For riser (1-2) and downcomer (3-4) section:

$$0 = \left(\frac{d_i}{L_t}\right) \frac{1}{\mathrm{Re}_{ss}\,\mathrm{Pr}_{ref}} \frac{\partial}{\partial \hat{z}} \left(\hat{\lambda}_w \frac{\partial \theta_w}{\partial \hat{z}}\right) - St_{mi} R_i \left(\theta_w - \theta_f\right) - St_{ma} R_o \left(\theta_w - \theta_a\right) \quad (13c)$$

6. Coolant

Coolant energy equation (9) can be presented as:

$$\hat{G}_c \hat{C}_{pc} \frac{\partial \theta_c}{\partial \hat{z}} = \left(\frac{d_i}{L_t}\right) \frac{1}{\mathrm{Re}_{ss}\,\mathrm{Pr}_{ref}} \frac{\partial}{\partial \hat{z}} \left(\hat{\lambda}_c \frac{\partial \theta_c}{\partial \hat{z}}\right) + St_{mex} R_{ex} \left(\theta_w - \theta_c\right) \quad (14)$$

The following non-dimensional numbers are used in these equations:

$$\mathrm{Re}_{ss} = \frac{G_{ss} d_i}{\mu_{ref}}, \mathrm{Pr}_{ref} = \frac{\mu_{ref} C_{pref}}{\lambda_{ref}},$$
$$Gr_m = \frac{g \beta_{av} \dot{Q} H \rho_{ref}^2}{A_{cs} C_{pref}} \left(\frac{d_i}{\mu_{ref}}\right)^3, \quad (15)$$
$$St_{mi} = \left(\frac{4 L_t}{d_i}\right) \frac{Nu_i}{\mathrm{Re}_i\,\mathrm{Pr}_i}, St_{mex} = \left(\frac{4 L_t}{d_i}\right) \frac{Nu_{ex}}{\mathrm{Re}_{ex}\,\mathrm{Pr}_{ex}},$$
$$St_{ma} = \left(\frac{4 L_t}{d_i}\right) \frac{h_a}{\rho_{pref} C_{pref} U_{ss}}$$

The area ratios are given by,

$$R_i = \frac{d_i^2}{d_o^2 - d_i^2}, R_o = \frac{d_o^2}{d_o^2 - d_i^2}, R_{ex} = \frac{d_o^2}{d_{ex}^2 - d_o^2} \quad (16)$$

E. Friction Factor and Heat Transfer Correlations

It has been repeatedly highlighted in literature that actual frictional pressure loss in NCLs greatly exceeds that predicted by the use of standard forced flow correlations developed for pipe flows [20], [21] and dedicated correlations are required for accurate assessment of friction. Considering this, several relations have been proposed and employed by various researchers for NCLs; however, the one developed by [20] for rectangular NCLs has been validated over the largest database and is given by:

$$f = 22.26 \left(\mathrm{Re}_d\right)^{-0.6744} \quad (17)$$

The most common heat transfer correlation is given by Dittus and Boelter [8]. It has been observed that, unlike friction factor, no suitable heat transfer relation is available which has been developed exclusively for NCLs. Hence, in the present work, Petukhov correlation with Gnielinski [25] modification is used for estimating the heat transfer coefficients for the fluid streams under turbulent condition (Re > 2300).

$$Nu_d = \frac{h_d L}{\lambda} = \frac{\left(f/8\right)\left(\mathrm{Re}_d - 1000\right)\mathrm{Pr}}{1 + 12.7\left(f/8\right)^{1/2}\left(\mathrm{Pr}^{2/3} - 1\right)} \quad (18)$$

where, the friction factor needs to be estimated by the Petukhov relation as follows:

$$f = \left[0.79 \ln\left(\mathrm{Re}_d\right) - 1.64\right]^{-2} \quad (19)$$

This correlation is reported to have an error margin of ±10% over a wide range of values ($2300 \le \mathrm{Re_d} \le 5 \times 10^6$ and $0.5 \le \mathrm{Pr} \le 2000$) and hence has successfully found extensive application in recently reported studies related to refrigeration and heat exchanger research, in particular [5], [6].

Specified heat transfer coefficient values for laminar flow (Re≤2300) has been defined based on the following correlation [28] as:

$$Nu_d = \frac{h_d L}{\lambda} = \begin{matrix} 1.86 \left(\mathrm{Re}_d\,\mathrm{Pr} \frac{d}{L_t}\right)^{1/3} \left(\frac{\mu_f}{\mu_{bulk}}\right)^{0.14} for Gz > 10 \\ 3.66 for Gz \le 10 \end{matrix} \quad (20)$$

Friction factor for Laminar flow is given by,

$$f = 64/\mathrm{Re}_d \quad (21)$$

and, Graetz number is defined as,

$$Gz = \left(\pi d / 4 L_t\right) \mathrm{Re}_d\,\mathrm{Pr} \quad (22)$$

Finally, the above correlations are derived for the flow through the duct or channel, not for annulus. Hence the correction factor is introduced for annular flows as:

$$h_{ex} = h_o 0.86 \left(\frac{d_c}{d_o}\right)^{0.16} \quad (23)$$

where, d_c and d_o are the outer diameter and inner diameter of the coolant annulus, respectively.

For estimation of wall-to-air heat transfer coefficient, riser and downcomer tubes can be considered as vertical cylinders. Due to the absence of any widely recognized correlation for natural convection in vertical cylinders, the correlation proposed by Churchill and Chu [23] for a vertical flat plate has been employed.

$$Nu_a = \frac{h_a L}{\lambda} = \left[0.825 + \frac{0.387 Ra_L^{1/6}}{\left[1+(0.492\mathrm{Pr})^{9/16}\right]^{8/27}}\right]^2 \quad (24)$$

where Ra_L is the associated Rayleigh number for convection to air over that length and it is estimated using properties of air corresponding to ambient temperature (T_a).

When the riser and downcomer sections are insulated, heat is transferred through the conductive resistance of insulating material and the convective resistance between the outer surface of insulation and air. Under such cases, effective heat transfer coefficient can be estimated as:

$$\frac{1}{h_a} = \frac{1}{h_a} + \frac{\delta_{ins}}{\lambda_{ins}} \quad (25)$$

where, δ_{ins} is thickness of insulation and λ_{ins} is thermal conductivity of insulating material.

F. Selection of Reference Parameter

As the system of governing equations is in non-dimensional form, choice of reference temperature (T_{ref}) becomes significant. All the properties need to be estimated at T_{ref} and magnitudes of dimensionless groups depend strongly on it. Hence, the prediction of non-dimensional form is inherently coupled with the selection of T_{ref}. Of course, the dimensional form of predicted results is completely independent of it. Generally, the coolant inlet temperature is expected to be the lowest in the entire system and that can be a reasonable choice as reference. For supercritical CO_2 under study, the base case for loop pressure is considered to be 90 bar. Cooling water inlet temperature is considered as reference temperature [5], [6]. Here it is taken as 313K i.e. the corresponding pseudo-critical temperature at 90 bar, to ensure that the property of CO_2 anywhere in the loop does not fall in the compressed liquid zone. Coefficient of thermal expansion, dynamic viscosity, specific heat and thermal conductivity are calculated at loop averaged temperature.

G. Estimation of Thermo–Physical Properties of CO2 and Water

Property estimation is an important component for accurate simulation of any natural circulation based device, as the flow is initiated and sustained by thermally-induced density gradient. The NIST standard reference database REFPROP is built within the MATLAB code, which is employed for calculating required thermodynamic and transport properties of CO2, as well as water for each node. Properties of the wall material and air have been taken from curve fitting the values at different temperatures from standardized property tables.

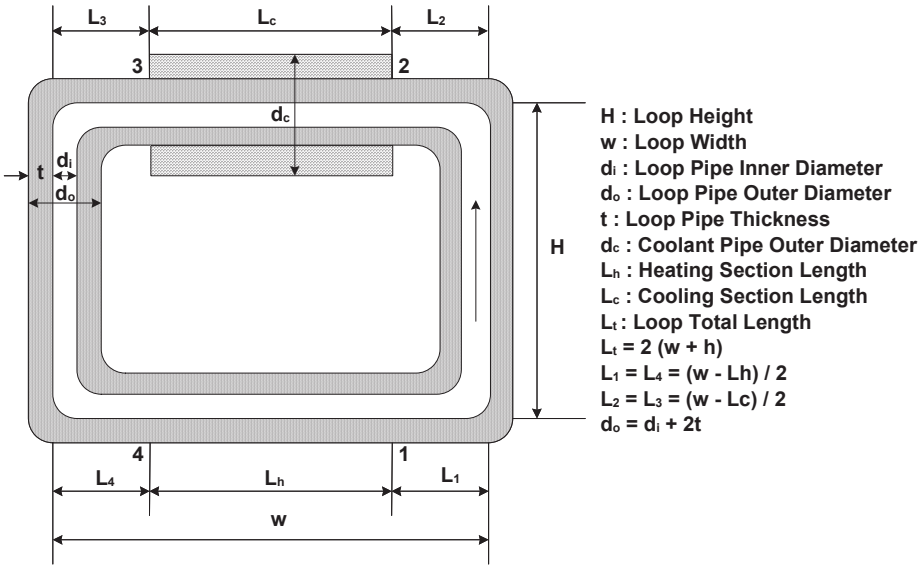

Fig. 2 Loop schematic dimension

H.Loop Dimension

Fig. 2 shows the nomenclature of the different dimension of the rectangular NCL considered in the present study.

The selected base cases for present study are as follows: Pressure = 90 bar, CW flow = 0.1 kg/s, CW inlet Temp = 313

K, Ambient Temp = 303 K, di = 7.68 mm, t = 3.02 mm, do = 13.72 mm (1/4 " Sch. 80), dc = 18.85 mm (3/4 " Sch. 80), H = 2 m, w = 1.5 m, Lh = 1.2 m, Lc = 1.2 m, Lt = 7 m, Pipe Material: AISI 316.

I. Numerical Solution Procedure

Simultaneous solution of the set of coupled equations along with the frictional and heat transfer correlations and property evaluation functions illustrate the complete system. One dimensional finite volume technique is employed [5], [6] to obtain the temperature profile for the loop fluid, wall material and coolant stream along with flow velocity. The power input to the system and the flow rate and inlet temperature of the cooling stream provide the external controlling parameters. The general solution strategy constitutes of assuming the steady-state flow rate as initial guess and employing that to find the values of characterizing dimensionless groups. That is employed to solve the steady-state version of the energy equations. The cyclic nature of the loop ensures that the last point of the flow path essentially merges with the first point, providing an improved value for the temperature. Proceeding with such an inner iteration, a converged temperature profile can be obtained for the assumed flow rate, which can, in turn, be corrected using the loop momentum equation in an outer iteration to get a converged pressure profile. Optimum number of grid points and convergence criteria have been determined through a trade-off between desired level of accuracy and solution time requirement. The entire procedure is then repeated until a fully converged solution is obtained having an accuracy level of 10^{-6} for temperature and 10^{-5} for pressure.

III. Results and Discussions

Mass flow rate of the loop fluid is plotted against different heater power levels (Fig. 3). It is seen that the steady state mass flow rate initially increases with power level attaining a peak near 1.5 kW. This can be denoted as buoyancy dominated region (BDR). Following the peak, the mass flow rate starts decreasing with increase in power input indicating a friction dominated region (FDR). Since the temperature rise is inversely proportional to mass flow rate, increasing the power input beyond the peak is not preferable.

Fig. 4 shows the steady state temperature profile for the loop fluid, wall and coolant at a power level of 1 kW. But the wall, having high thermal conductivity, shows a steep temperature variation at the entry and exit of the heating and cooling sections. Coolant shows very little temperature variation (<5K) across the cooler due to the large flow rate and specific heat of water.

Fig. 5 shows the steady state pressure profile along the non-dimensional loop length exhibiting quite modest variation (6 kPa). Loop pressure decreases in the hot leg (riser) section and increases the same way in the cold leg (downcomer). The net friction loss over the entire loop length is gained by the buoyancy effect induced by the change in density due to temperature difference in the riser and downcomer sections.

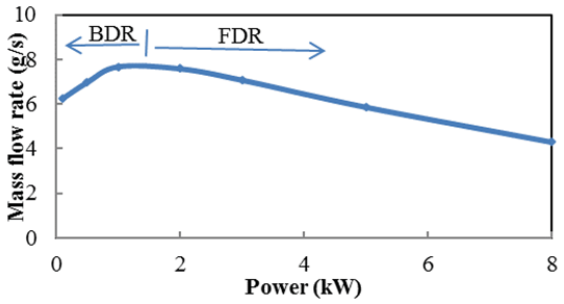

Fig. 3 Mass flow rate at different input power

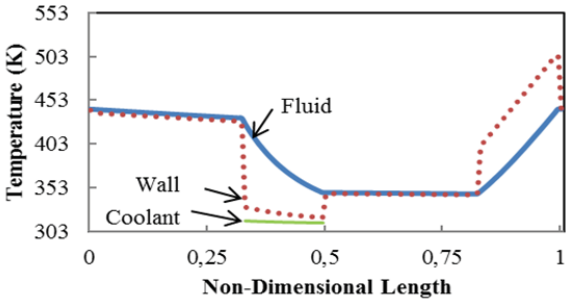

Fig. 4 Steady state temperature profile along the loop length

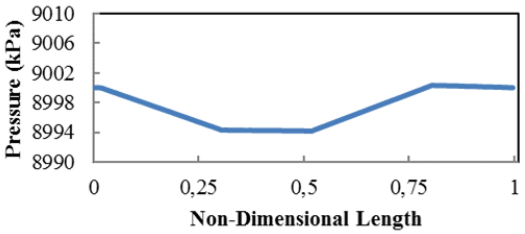

Fig. 5 Steady state pressure profile along the loop length

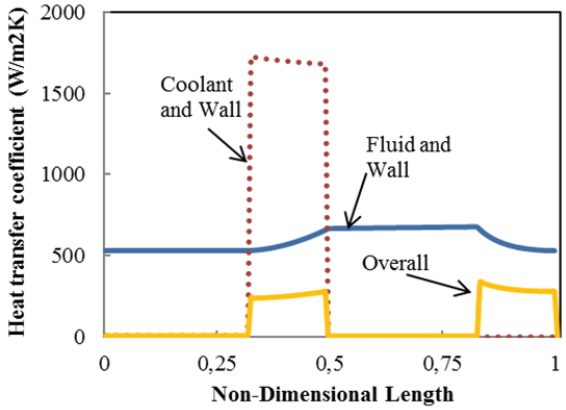

Fig. 6 Heat transfer coefficients along the loop length

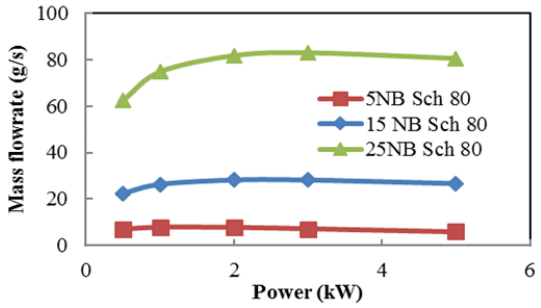

Fig. 7 Effect of loop diameter on mass flow rate

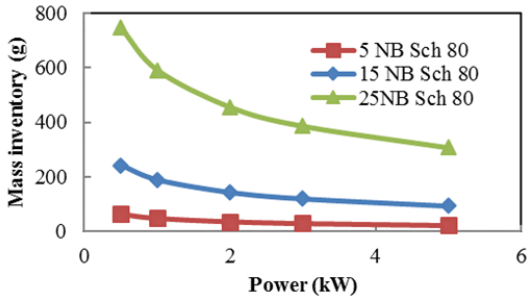

Fig. 8 Effect of loop diameter on mass inventory

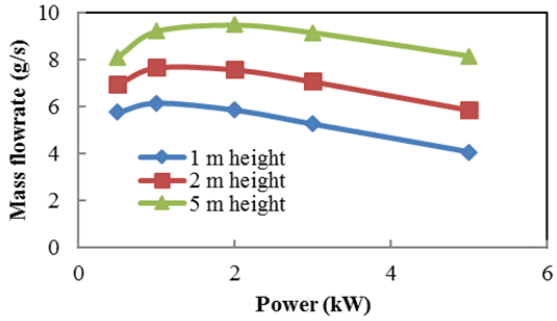

Fig. 9 Effect of loop height on mass flow rate

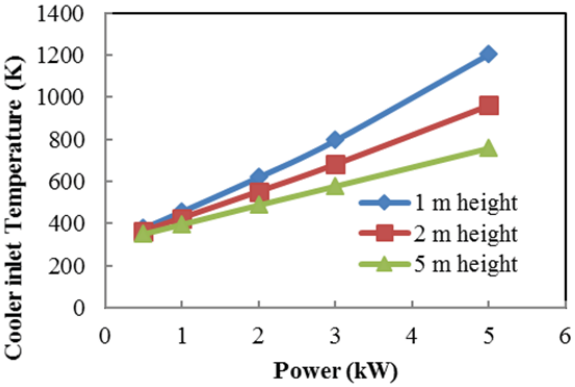

Fig. 10 Effect of loop height on cooler inlet temperature

Heat transfer coefficients at the inner and outer surfaces, along with overall heat transfer coefficient, are plotted along the loop length (Fig. 6). Coolant, being water, yields a higher heat transfer coefficient than the loop fluid CO_2.The inner surface heat transfer coefficient value increases along the cooling section and decreases along the heating section. The un-insulated area (riser and downcomer) exposed to ambient air at the outer surface shows very low heat transfer due to natural convection. The overall heat transfer coefficient in the heater sections is high since the resistance to heat transfer is only due to the wall and the inner convective heat transfer, whereas the overall heat transfer coefficient is high in cooler due to high external heat transfer coefficient.

A. Effect of Loop Diameter

Inner diameter of the loop is an important parameter with respect to practical issues such as space requirement and manufacturing costs. Increase in diameter increases the cross-sectional area much more than the increase of mass flux leading to a net reduction in velocity and hence frictional resistance. Thus, for the same power input, a larger inner diameter yields a higher mass flow rate. It is also observed that the region for gravity dominated zone increases with pipe size. The peak value of mass flow rate shifted from 1.5kW for 5 NB Sch80 (ID/OD:7.68/13.72 mm) to 2kW for 15NB Sch80 (ID/OD: 13.88/21.34 mm) and 3 kW for 25NB Sch80 (ID/OD:24.3/33.4 mm) i.e. yielding higher power level with increase in pipe size (Fig. 7).

For a particular power level, higher pipe size yields higher internal volume, thereby the CO2mass inventory increases significantly (Fig. 8). Higher mass flow rate reduces the average fluid temperature causing increase in density, but this has marginal impact on mass inventory.

For a particular diameter, as power increases average loop temperature increases, thereby density reduces, which gives lower mass inventory. Larger diameter is better considering the loop mass flow rate, but the response to transient study is required as the higher mass inventory may reduce the transient stability.

B. Effect of Loop Height

The driving force in any vertical rectangular NCL is the difference in density of the working fluid flowing in vertical arms, and hence loop height plays a decisive role in generating the required buoyancy force. The effect of height on buoyancy is clearly shown from the mass flow rate graph. With the increasing power input the mass flow rate starts increasing, reaches a peak and then starts decreasing. The same pattern is visible here, but with increasing height the peak shifts to the right (Fig. 9). Though increase of height increases the loop length and hence friction, but the buoyancy effect is more pronounced than frictional drop; as a result, buoyancy dominated region increases with the increase of height. Hence, the taller loop is better as it increases the driving force. But the effect is more with the increase of diameter, as the internal volume changes faster with the diameter compare to the height. For a given internal volume and at a particular power level, higher mass flow rate can be achieved very easily by increasing diameter than to increasing the height.

As input power increases, the temperature throughout the loop increases as indicated by the cooler inlet temperature shown in Fig. 10. The reduced temperature at the cooler inlet

of taller loops at higher power is due to the increased mass flow rate for the taller loop.

Loop effectiveness can be defined as:

$$\varepsilon_{NCL} = \frac{Q_{CW}}{Q_{in}} = 1 - \frac{Q_{loss}}{Q_{in}} \quad (26)$$

C. Effect of Ambient Temperature and Insulation

It is quite obvious that with the application of insulation, heat leakage through the wall can be reduced drastically. Considering glass fibre (0.046 W/mK) as the insulating medium, amount of heat transferred to coolant stream increases with the increase of insulation thickness for a particular ambient temperature. The effect is more pronounced for warmer ambient temperature as it leads to better effectiveness for any particular insulation thickness (Fig. 11).

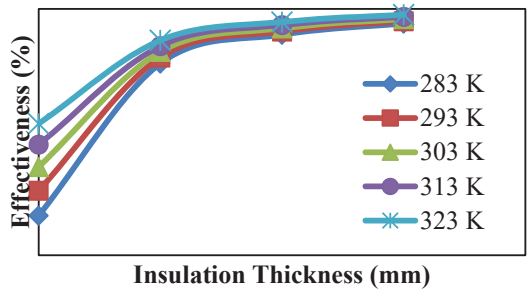

Fig. 11 Effect of insulation thickness on loop effectiveness

Fig. 12 shows the effectiveness at different diameter and different input power level for a constant ambient temperature of 303 K. It is clear that for the 15 NB pipe the heat loss is less as the surface area is less compare to that of 25 NB pipe for each power level. For a particular diameter pipe, higher input power gives lower effectiveness for un-insulated case, but the effect is almost negligible even at 25 mm insulation thickness.

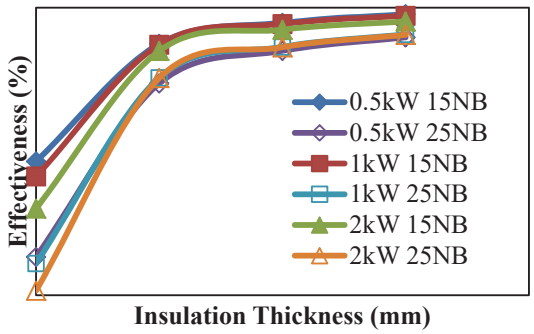

Fig. 12 Effect of diameter and power level on loop effectiveness

IV. Conclusion

Steady state numerical simulation studies have been carried out on CO_2 based NCL at various operating conditions. Supercritical phase CO_2 at an operating pressure of 90 bar is taken as the loop fluid for an input power varying between 0.5 kW to 6 kW. Studies are carried out for various loop diameters, loop heights, and heating/cooling lengths. Conclusions from the simulation results can be summarized as follows:

1. For a given loop, as the power input at the heater increases, the loop fluid mass flow rate increases initially (gravity dominated region), reaches a peak and then starts decreasing (friction dominated region). Wall and fluid temperature profiles closely match together except at heating and cooling sections, where wall material temperature responds much faster to the heater or cooler. For the operating conditions considered, there is very little pressure drop in the loop with maximum value of 6 kPa which is less than 0.1% of the loop pressure.
2. As the loop diameter increases, the mass flow rate increases for a particular power level due to less resistance to flow. However, the mass inventory increases due to higher internal volume of the loop, which may give rise to safety concerns in view of the high operating pressure. In addition, the transient response of the loop is also affected due to the increased mass. Thus, there is a need for trade-off between steady state performance and the practical constraints related to safety and response.
3. As the loop height increases, the heat loss to ambient also increases leading to a smaller fraction of energy transfer from source to sink (i.e. less effectiveness). But as the height increases buoyancy also increases leading to an increase in the range of buoyancy dominated region i.e. peaks of mass flow rate shifted towards the higher power level. Also mass flow rate increases as the loop height increases, which in turn reduces the loop temperature at the heater outlet or cooler inlet for the taller loop.
4. As the ambient temperature increases, the heat loss from the high temperature NCL to ambient reduces, increasing loop effectiveness. The fully insulated case (no heat loss) leads to a higher temperature profile as expected throughout the loop compared to that of heat loss case. As the thickness of insulation increases the effectiveness increases but the effect is reduced thereafter reaching a maximum value.

References

[1] A.K. Yadav, MRamgopal, S. Bhattacharyya, CFD analysis of CO2based natural circulation loop with end heat exchangers, Appl. Therm. Eng., 36 (2012a) 288-295

[2] B.T. Swapnalee, P.K. Vijayan, M. Sharma, D.S. Pilkhwal, Steady state flow and static instability of supercritical natural circulation loops, Nucl.Eng. and Des., 245 (2012) 99–112.

[3] D.B. Kreitlow, G.M. Reistad, Themosyphon models for downhole heat exchanger application in shallow geothermal systems, J. Heat Transfer 100 (1978) 713–719.

[4] D.E. Kim, M.H. Kim, J.E. Cha, S.O. Kim. Numerical investigation on thermal–hydraulic performance of new printed circuit heat exchanger model, Nucl. Eng. Des. 238 (2008) 3269–3276.

[5] D.N. Basu, S. Bhattacharyya, P.K. Das, Effect of geometric parameters on steady-state performance of single-phase NCL with heat loss to ambient, Int. J. Therm. Sci. 47 (2008) 1359–1373.

[6] D.N. Basu, S. Bhattacharyya, P.K. Das, Effect of heat loss to ambient on steady-state behaviour of a single-phase natural circulation loop, Int. J. Therm. Sci. 24 (2007) 1432–1444.
[7] F.C.V.N. Fourie, C.E. Schwarz, J.H. Knoetze, Phase equilibria of alcohols in supercritical fluids Part I. The effect of the position of the hydroxyl group for linear C8 alcohols in supercritical carbon dioxide, J. Supercrit. Fluids 47 (2008) 161–167.
[8] F.W. Dittus, L.M.K. Boelter, Heat transfer in automobile radiators of tubular type, University of California Publications in Engineering, 2 (1930) 443–461.
[9] H. Yamaguchi, X.R. Zhang, K. Fujima, Basic study on new cryogenic refrigeration using CO2 solid–gas two phase flow, Int. J. Refrig. 31 (2008) 404–410.
[10] K.E. Torrance, Open–loop thermosyphons with geological application, J. Heat Transfer 100 (1979) 677–683.
[11] K. Kiran Kumar, M. Ram Gopal, Carbon dioxide as secondary fluid in natural circulation loops, Proc. IMechE, Part E: J. Process Mech. Engg. 223 (2009a) 189-194.
[12] K. Kiran Kumar, M. Ram Gopal, Steady-state analysis of CO2 based natural circulation loops with end heat exchangers, Appl. Therm. Eng. 29 (2009b) 1893–1903
[13] K. Ochsner, Carbon dioxide heat pipe in conjunction with a ground source heat pump (GSHP), Appl. Therm. Eng. 28 (2008) 2077–2082.
[14] K. Wang, E. Magnus, H. Yunho, R. Radermacher, Review of secondary loop refrigeration system, Int.J.of Refrigeration, 33 (2010) 212–234.
[15] L. Chen, X.-R. Zhang, H. Yamaguchi, Z.-S. (Simon) Liu, Effect of heat transfer on the instabilities and transitions of supercritical CO2 flow in a natural circulation loop, Int. J. Heat Mass Transf. 53 (2010) 4101–4111.
[16] M.H. Kim, J. Pettersen, C.W. Bullard, Fundamental process and system design issues in CO2 vapor compression systems, Progress in Energy and Combustion Science, 30 (2004) 119–174.
[17] M. Ishii, I. Kataoka, Scaling laws for thermal-hydraulic system under single phase and two-phase natural circulation, Nucl. Eng. and Des., 81 (1984) 411-425.
[18] M. Misale, P. Garibaldi, J.C. Passos, G.D. Bitencourt, Experiments in a single phase natural circulation mini-loop, Experimental Thermal and Fluid Science, 31 (2007) 1111–1120.
[19] P. Bondioli, C. Mariani, E. Mossa, A. Fedelli, A. Muller, Lampante olive oil refining with supercritical carbon dioxide, J. Am. Oil Chem. Soc. 69 (1992) 477–480.
[20] P.K. Vijayan, H. Austregesilo, Scaling laws for single-phase natural circulation loops, Nucl. Eng. and Des., 152 (1994)331–347.
[21] P.K. Vijayan, Experimental observations on the general trends of the steady state and stability behaviour of single phase natural circulation loops, Nucl. Eng. and Des., 215 (2002) 139–152.
[22] S.K. Mousavian, M.Misale, F. D'Auria, M.A. Salehi, Transient and stability analysis in single phase natural circulation, Annals of Nuclear Energy, 31 (2004) 1177-1198.
[23] S.W. Churchill, H.H.S. Chu, Correlating equations for laminar and turbulent free convection from vertical plate, Int. J. Heat Mass Transfer 18 (11) (1975) 1323–1329.
[24] Dostal, P. Hejzlar, M.J. Driscoll, The supercritical carbon dioxide power cycle: comparison to other advanced power cycles, Nucl. Technol. 154 (2006) 283–301.
[25] Gnielinsky, New equation for heat and mass transfer in turbulent pipe and channel flow, Int. Chemical Engineering, 16 (1976) 359-368.
[26] X. Zhang, L. Chen, H. Yamaguchi, Natural convective flow and heat transfer of supercritical CO2 in a rectangular circulation loop, Int. J. Heat and Mass Transfer 53 (2010) 4112–4122.
[27] Y. Zvirin, A review of natural circulation loops in pressurizes water reactors and other systems, Nucl. Eng. And Des., 67 (1981) 203–225.
[28] B.T. Nijaguna, Thermal Sciences/Engineering Data Book, Allied Publishers Limited, New Delhi, 1992, pp. K-13.